# Evaluation of Nonlinear MIMO Controllers for Independent Metering in Mobile Hydraulics

Lukas Bachmann, André Sitte, Jürgen Weber

*Chair of Fluid-Mechatronic Systems*
*Technische Universität Dresden*
*Dresden, Germany*
*lukas.bachmann@tu-dresden.de, fluidtronik@mailbox.tu-dresden.de*

Hydraulic cylinder drives with coupled control edges suffer from inherent losses due to dependent meter-in and meter-out flow control. Velocity and pressure demands with different valve opening requirements collide and result in energy dissipation at the control edges. Independent metering technology provides individual actuation of inlet and outlet valves and leads to higher efficiency. The additional control input offers separate control of cylinder velocity, i.e. flow, and chamber pressure. However, the resulting nonlinear Multiple Input Multiple Output (MIMO) system poses several challenges for the control algorithm. Cross coupling between the system states requires multivariable control. Furthermore, the commonly used linearization approaches strongly depend on the current operating point of the hydraulic system. In mobile application, these operating points are usually difficult to predict and move across a wide range. Therefore, a nonlinear, multivariable control algorithm is required. This paper presents some frequently discussed nonlinear control approaches, namely flatness-based tracking control, sliding mode control and exact input/output linearization, and evaluates their performance and applicability in the mobile hydraulic context. Control variables are velocity and weighted chamber pressure of the cylinder. Previous research on these controller concepts showed promising results for simple nonlinear MIMO systems. However, more complex systems, incorporating modelling uncertainties and limited observability have rarely been studied thoroughly. Therefore, this study focuses on the validation of the controller implementa-

*River Journal,* 1–18.

tion based on simplified models of a hydraulic valve-controlled manipulator with two joints. This is followed by an investigation of the performance on increasingly sophisticated and realistic models. Assessment criteria are robustness against parameter and model uncertainties, computational efficiency, communication delay and measurement effort.

**Keywords:** Nonlinear Control Theory, Flatness-based Control, Sliding Mode Control, Exact Input/Output Linearization, Independent Metering, Hydraulic Manipulator.

## 1 Introduction

The progress of automation and the demand for energy efficient hydraulic systems brings valve structures with decoupled control edges for independent flow and pressure control into focus. This principle is known for several decades as Independent Metering (IM). Past research at the Institute of Fluid-Mechatronic Systems [1, 2] has shown high energy saving potentials. Yet the technology has barely entered today's construction sites [3]. Main reason for the Original Equipment Manufacturer's (OEM) hesitancy is the increased control engineering effort and accompanying cost-intense sensor and valve equipment.

Hence, this paper seeks to evaluate some frequently discussed control strategies for the application in mobile hydraulic systems using IM technology. Given high pressure on costs and limited computational resources in mobile machinery, the realization and implementation is analyzed and questioned.

The control task of valve controlled hydraulic cylinder drives with IM-valve technology can be described as a nonlinear MIMO system. Sitte et al. [4, 5] analyze the decoupling effect of individual pressure compensators (IPC) on intrinsic coupling for the application of Single Input Single Output (SISO) controllers. The authors identified reduction of the coupling factor due to the usage of IPCs but also detected a strong dependency on the current state of operation. Thus, the applicability of SISO controllers is limited and multivariable control algorithms are required.

One strategy to control nonlinear systems is through nonlinear decoupling and linearization by feedback [6–9]. This is a simple and straight-forward solution which achieves good results if and only if the systems characteristic are known to a certain degree. Unknown or inaccurate system knowledge as well as parameter uncertainties will result in insufficient compensation of the systems nonlinearities and consequently poor performance.

The lack of robustness can be overcome by the introduction of so-called sliding surfaces [10]. The sliding mode controller (SMC) is motivated by the fact that a first degree system is easier controllable than a $n^{\text{th}}$ order system described by $n^{\text{th}}$ order differential equations [11]. The transformation is done by attracting the system states toward a hyperplane or sliding surface, along which the system states are stabilized to a desired equilibrium state or trajectory.
Discontinuous switching laws reached good control performance for systems with model and parameter uncertainties [9, 12]. Unfortunately the use of such switching laws excites high frequency oscillations, known as the chattering phenomenon. This may result in premature aging or even damaging of the control actuators and can excite unmodeled high-frequency dynamics. Piecewise-continous switching laws [11–13] achieved slightly better performance and reduced strain on band-width limited actuators. The states are no longer drawn infinetisemally close towards the sliding surface but pulled inside a finite and bounded neighborhood.
The most promising results though were obtained using higher order sliding modes (HOSM) [14–20]. Beside the requirement to minimize the distance i.e. sliding variable $s$ to the sliding surface, restrictions on the derivatives $s^{(n)}$, such as $s^{(n)} = 0$, are applied so that discontinuities appear at the $n$+1-th derivative at the earliest. This concept is known as the super twisting sliding mode controller (STSMC).
For a certain class of nonlinear systems another powerful control approach can be implemented. Exploiting the system characteristic of differential flatness [21] a dynamic, stabilizing state feedback can be realized by reconstructing the system states through a flat output $y$.

**Definition 1.1.** A system is called differentially flat if, and only if, a tuple of differentially independent quantities exists from which all other quantities of the system can be calculated without solving a differential equation. Such a tuple is called flat output.

Although Def. 1.1 seems restrictive, many physical systems meet these requirements and flatness-based tracking controllers (FTC) have been developed for various applications, among them hydraulic systems [1, 22–24].

## 2 System description

For the model-based controller design we consider the hydraulic system depicted in Fig. 1. The valve structure consists of two 2/2 leak-proof proportional valves and one 4/3 switching valve. The latter is used for flow reversal at negative speeds while the proportional valves control pressure and cylinder velocity.

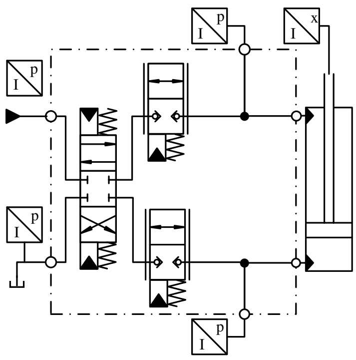

Figure 1 IM valve-controlled cylinder with sensor information

The force equilibrium at the hydraulic cylinder is given by

$$\mathrm{m_{cyl}} \cdot \ddot{z} + \mathrm{d_{cyl}}\left(\dot{z}\right) \cdot \dot{z} + F_{\mathrm{L}} = p_{\mathrm{A}} \cdot A_{\mathrm{A}} - p_{\mathrm{B}} \cdot A_{\mathrm{B}} \tag{1}$$

where $F_{\mathrm{L}}$ denotes the unknown load force at the mechanical connector of the cylinder. For the controller design the damping $d_{\mathrm{cyl}}$ is assumed linear proportional with respect to the cylinder velocity.
The pressure gradient inside the oil-filled volumes is expressed by

$$\dot{p}_{\mathrm{A}} = \frac{K'}{V_{\mathrm{A}} + A_{\mathrm{A}} z}\left(Q_{\mathrm{A}} - \mathrm{A_A}\dot{z}\right) \tag{2a}$$

$$\dot{p}_{\mathrm{B}} = \frac{K'}{V_{\mathrm{B}} + A_{\mathrm{B}}\left(h - z\right)}\left(\text{-}Q_{\mathrm{B}} + \mathrm{A_B}\dot{z}\right). \tag{2b}$$

For simplification the pressure-induced expansion of the piping system and the temperature influence on the bulk modulus $K'$ are neglected. The pipe volumes $V_{\mathrm{A}}$ and $V_{\mathrm{B}}$ are constant while the variation of the chamber volume and the associated impact on the systems eigenfrequency and damping is considered.
We assume turbulent flow inside the valves and thereby define the flow characteristic with the following equation:

$$Q_i = K_{\mathrm{V}}(y_i) \cdot \mathrm{sign}\left(\Delta p_i\right) \sqrt{|\Delta p_i|}. \tag{3}$$

The opening gradient $K_\mathrm{V}$ of the valve orifice depends on the valve's nominal flow characteristic and on the normalized valve spool position $y_i$. For invertibility this is described as a polynomial curve and (3) is fitted to the valve characteristic depicted in Fig. 3.
Valve dynamics are neglected for the controller design. Especially in the case of large mobile machinery the dynamics of the kinematic chain are much slower than the valve dynamics.

## 3 Controller Design

Based on the system description we implemented four different control strategies. The control task involves velocity and pressure control. Since the control inputs can control two system states, only one chamber pressure is controllable. In order not to change the controlled state depending on the load situation, we introduce the weighted chamber pressure

$$p_\mathrm{K} = \frac{p_\mathrm{A} \cdot p_\mathrm{B}}{p_\mathrm{A} + p_\mathrm{B}} \tag{4}$$

as control variable in addition to the cylinder speed.

### 3.1 Exact Input/Output Linearization

With the definition of the state vector

$$\boldsymbol{x} = [\dot{z} \quad p_\mathrm{A} \quad p_\mathrm{B}]^\mathsf{T} \tag{5}$$

and output mapping using (4)

$$\boldsymbol{h}(\boldsymbol{x}) = [\dot{z} \quad p_\mathrm{K}]^\mathsf{T} \tag{6}$$

the simplified system governed by (1) to (3) can be represented as a nonlinear control-affine system of the form

$$\dot{\boldsymbol{x}} = \boldsymbol{f}(\boldsymbol{x}) + \boldsymbol{G}(\boldsymbol{x})\boldsymbol{u} \tag{7a}$$
$$\boldsymbol{y} = \boldsymbol{h}(\boldsymbol{x}) \tag{7b}$$

where the system state $\boldsymbol{x}$, the input $\boldsymbol{u}$ and output $\boldsymbol{y}$ are $n = 3$, $p = 2$ and $m = 2$ dimensional. The smooth vector fields $\boldsymbol{f}$ and $\boldsymbol{h}$ denote the autonomous part of the system and the output mapping. $\boldsymbol{G}$ is the square matrix-valued control sensitivity with according dimensions.

With exact input/output linearization, the nonlinearity of the system is compensated by an inverse, nonlinear control law. For this, the system output must be derived until at least one of the system inputs comes up:

$$y_i^{(r_i)} = \pounds_{\boldsymbol{f}}^{r_i} h_i + \sum_{j=1}^{m} \pounds_{\boldsymbol{g}_i} \pounds_{\boldsymbol{f}}^{r_i - 1} h_i u_j \tag{8}$$

**Definition 3.1.** The derivation degree $r_i$ for which

$$\pounds_{\boldsymbol{g}_i} \pounds_{\boldsymbol{f}}^{r_i - 1} \neq 0 \wedge \pounds_{\boldsymbol{g}_i} \pounds_{\boldsymbol{f}}^{k} = 0, \quad k \in \{0, \ldots, r_i - 2\}$$

holds, is called relative degree [25]. $\boldsymbol{g}_i$ are the row vectors of $\boldsymbol{G}$.

For a MIMO system this is explicitly shown in (9), where $\boldsymbol{G}^*$ is called decoupling matrix [25].

$$\begin{bmatrix} y_1^{(r_1)} \\ \vdots \\ y_m^{(r_m)} \end{bmatrix} = \begin{bmatrix} \pounds_{\boldsymbol{f}^{r_1}} h_1 \\ \vdots \\ \pounds_{\boldsymbol{f}^{r_m}} h_m \end{bmatrix} + \begin{bmatrix} \pounds_{\boldsymbol{g}_1} \pounds_{\boldsymbol{f}^{r_1 \text{-} 1}} h_1 & \cdots & \pounds_{\boldsymbol{g}_m} \pounds_{\boldsymbol{f}^{r_1 \text{-} 1}} h_1 \\ \vdots & \ddots & \vdots \\ \pounds_{\boldsymbol{g}_1} \pounds_{\boldsymbol{f}^{r_m \text{-} 1}} h_m & \cdots & \pounds_{\boldsymbol{g}_m} \pounds_{\boldsymbol{f}^{r_m \text{-} 1}} h_m \end{bmatrix} \boldsymbol{u}$$
$$\boldsymbol{y^r} = \boldsymbol{f}^* + \boldsymbol{G}^* \boldsymbol{u} \tag{9}$$

Exact input/output linearization is achieved by introducing the virtual control inputs $\omega_i$ and solving (9) for $\boldsymbol{u}$:

$$\boldsymbol{u} = (\boldsymbol{G}^*)^{-1} [\boldsymbol{\omega} - \boldsymbol{f}^*], \qquad \omega_i = y_i^{(r_i)}. \tag{10}$$

For the virtual inputs $\omega_i$, linear error dynamics can be specified according to the respective relative degree $r_i$. Thereby, the linearizing feedback is supplemented by a stabilizing one.
For the studied hydraulic system the corresponding relative degrees are $r_v = 2$ for velocity control and $r_{p_\mathrm{K}} = 1$ for pressure control. The linear error dynamics are thus stabilized by

$$\omega_v = \ddot{v}_\mathrm{d} \qquad -k_{v,1} (\dot{v} - \dot{v}_\mathrm{d}) - k_{v,0} (v - v_\mathrm{d}) \tag{11a}$$
$$\omega_{p_\mathrm{K}} = \dot{p}_\mathrm{K,d} \qquad -k_{p_\mathrm{K},0} (p_\mathrm{K} - p_\mathrm{K,d}) \tag{11b}$$

with all gains $k_{i,j} > 0$ as the necessary condition is also sufficient for first and second degree polynomial equations.

### 3.2 Sliding Mode Control

**Definition 3.2.** Consider the control-affine system (7). For each of the $m$ control variables we define a sliding surface of the kind:

$$s_i(\boldsymbol{z}, t) = \left(\frac{\mathrm{d}}{\mathrm{d}t} + \lambda_i\right)^{r_i - 1} \tilde{y}, \quad \lambda > 0, \quad i = 1, \cdots, m. \tag{12}$$

The relative degree $r_i$ is determined as described in Def. 3.1 and the positive constant $\lambda_i$ determines exponential convergence on $s_i$.

With two sliding surfaces as in Def. 3.2 for $v$ and $p_{\mathrm{K}}$ the decoupled $r_i^{\mathrm{th}}$-order system (9) can be transformed in two $1^{\mathrm{st}}$-order stabilization problems in $s_i$ [13]. In the $s_i$-space the relative degree is reduced to one, as the input per definition already appears after one derivation.
For an asymptotic attraction towards the sliding surface the positive definite and radially unbounded Lyapunov function

$$V_i(s_i) = \frac{1}{2} s_i^2 \qquad\qquad \dot{V}_i(s_i, \dot{s}_i) = \frac{1}{2}\frac{\mathrm{d}}{\mathrm{d}t}\left(s_i^2\right) \overset{!}{<} 0 \tag{13}$$

is chosen. In order to reach $s_i$ in finite time $t \leq |s_i(0)| / \eta_i$ [13], the following tightening of (13) shall apply:

$$\dot{V}(s_i, \dot{s}_i) = s_i \dot{s}_i \overset{!}{\leq} \text{-}\eta ||s_i||, \qquad\qquad \eta_i > 0. \tag{14}$$

The positive constant $\eta_i$ governs the attracting speed towards the sliding surface $s_i$. Inserting (9) in (14) results in an inequality equation which can be simplified by introducing a piecewise continuous discontinuous control law yielding

$$\boldsymbol{u} = (\boldsymbol{G}^*)^{\text{-}1} \left[\boldsymbol{\omega} - \boldsymbol{f}^* - \boldsymbol{k} \cdot \mathrm{sat}(\boldsymbol{s}/\boldsymbol{\epsilon})\right] \tag{15}$$

where the virtual control input equals $\omega_i = s_i - y_i^{(r_i)}$.
The additional parameter $\epsilon$ denotes the tolerance width around the sliding surface where no control action is performed to reduce chattering [13].
In contrast to the control strategy of 3.1 model uncertainties of the kind

$$\left|\tilde{f}_i^* - f_i^*\right| \leq F_i \tag{16a}$$

$$\boldsymbol{G^*} = (\boldsymbol{I} + \boldsymbol{\Delta})\tilde{\boldsymbol{G}}^* \tag{16b}$$

can be incorporated in (15) by solving

$$(1 - \delta_{ii})k_i + \sum_{j \neq i} \delta_{ij} k_j = F_i + \sum_{j=1}^{\mathrm{M}} \delta_{ij} \left|\omega_i^{(r_i - 1)} - \tilde{f}_i^*\right| + \eta_i \tag{17}$$

Table 1 Parametric uncertainties for valve controlled cylinder drive

| Parameter | Nominal Value | Range | |
|---|---|---|---|
| $F_{\mathrm{L}}$ | $0\,\mathrm{kN}$ | -40 kN | $\cdots$+80 kN |
| $K'$ | $14\,000\,\mathrm{bar}$ | $8000\,\mathrm{bar}$ | $\cdots 16\,000\,\mathrm{bar}$ |
| $\partial K_{\mathrm{V}}/\partial y^{\mathrm{a}}$ | $1.527 \times 10^{-4}\ \sqrt{\mathrm{m}^7/\mathrm{kg}}$ | $\pm 10\,\%$ | |
| $d_{\mathrm{cyl}}$ | $150\,\mathrm{kNs/m}$ | +75 kNs/m | $\cdots 300\,\mathrm{kNs/m}$ |
| $m_{\mathrm{cyl}}$ | $3000\,\mathrm{kg}$ | $2500\,\mathrm{kg}$ | $\cdots 3500\,\mathrm{kg}$ |

[a] For simplification the mean linear gradient is varied.

for $k_i$ as proposed by [9, 13]. The maximum relative deviations of $\boldsymbol{G}^*$ are denoted by $\delta_{ij} \geq |\Delta_{ij}|$.
For the given use case (Fig. 1) geometric quantities are considered well known while external influences like load force and pressure and temperature sensitive parameters like the bulk modulus are assigned with an uncertainty range denoted in Table 1.

### 3.3 Super Twisting Sliding Mode Control

Another approach to reduce chattering is the use of HOSM [14,15]. A second order implementation of HOSM is known as the STSMC.
Again sliding surfaces of relative degree $r_i = 1$ are defined according to (12) and decoupling and input assignment of the virtual control law is given by the inversion of the input sensitivity:

$$\boldsymbol{u} = (\boldsymbol{G}^*)^{-1} [\boldsymbol{\omega} - \boldsymbol{f}^*] . \tag{18}$$

Referring to possible implementations [14] of the virtual control input, we select the following system of differential equations for $\boldsymbol{\omega}$:

$$\omega_i = -k_{i,1}\sqrt{|s_i|}\mathrm{sign}\,(s_i) - k_{i,2}s_i + \Omega_i \tag{19a}$$

$$\dot{\Omega}_i = k_{i,3}\mathrm{sign}\,(s_i) - k_{i,4}s_i . \tag{19b}$$

There exist publications [14, 18, 26] considering the estimation of the control parameters $k_{i,j}$ for robust stability against additive disturbances on (9). To the authors knowledge there has been no methodology do determine the gains $k_{i,j}$ for a class of parameter and model uncertainties like (16) thus, the parameters were determined empirically for this study.

### 3.4 Flatness-based Tracking Control

Exploiting the system property of flatness, as defined in Def. 1.1, the system can be stabilized and controlled along a reference trajectory by a state feedback law.

First, flatness must be proven for the considered system output (6). This is achieved by systematically expressing the system's states through a flat output $\boldsymbol{\eta}$ and its derivatives[1]. For the sake of clarity the following expressions are abbreviated and only the occurring derivation orders are listed.

$$x_1 = \psi_1(\eta_1) = \eta_1 \tag{20a}$$
$$x_2 = \psi_2(\eta_1, \dot{\eta}_1, \eta_2) \tag{20b}$$
$$x_3 = \psi_3(\eta_1, \dot{\eta}_1, \eta_2) \tag{20c}$$

(20a) follows directly from (6) and (20b) and (20b) result from rearranging (1) and inserting (6). Also the flow rate can be expressed by using the derivatives of (20b) and (20c) respectively with (2a) and (2b). Hence, it is proven that simply by measuring the system's flat output, all system states can be computed. The system is *input/state linearizable*[2] and consequently the required system input can be obtained for a desired system state expressed by $\boldsymbol{\eta}$:

$$u_\mathrm{A} = \varphi_1(\eta_1, \dot{\eta}_1, \ddot{\eta}_1, \eta_2, \dot{\eta}_2) \tag{21a}$$
$$u_\mathrm{B} = \varphi_2(\eta_1, \dot{\eta}_1, \ddot{\eta}_1, \eta_2, \dot{\eta}_2) \tag{21b}$$

Equation (21) can be considered as a feed forward control with the inverse system characteristic. To compensate disturbances and modeling uncertainties an additional control through state feedback is introduced. Choosing $\eta_i$ as new states $x'_i$ and the highest derivatives of $\eta_i$ as virtual control inputs $\omega_i$ a linear, classical[3] state space model in Brunovský normal form [22] is created where the highest derivatives of the flat output are chosen as virtual system

[1] The symbol $\boldsymbol{\eta}$ is used to distinguish the flat output from the general system output $\boldsymbol{y}$.

[2] For SISO systems this approach is in fact identical to the input/output linearization.

[3] As long as no derivatives of the system input $\boldsymbol{u}$ appear in (22) the state space model is classic and static state feedback can be implemented, otherwise dynamic feedback is mandatory [25].

inputs for the control law.

$$\dot{x}'_{1,1} = x'_{1,2} \qquad = \dot{\eta}_1 \tag{22a}$$

$$\dot{x}'_{1,2} = \varphi_1(x'_{1,1}, x'_{1,2}, x'_{2,1}, u) \qquad \stackrel{!}{=} \omega_1 \tag{22b}$$

$$\dot{x}'_{2,1} = \varphi_2(x'_{1,1}, x'_{1,2}, x'_{2,1}, u) \qquad \stackrel{!}{=} \omega_2 \tag{22c}$$

A linear, time-invariant error dynamics of the tracking error $\tilde{\boldsymbol{\eta}} = \boldsymbol{\eta} - \boldsymbol{\eta}_{\text{ref}}$ is specified for the virtual inputs.

$$\ddot{\tilde{\eta}}_1 + k_{1,1}\dot{\tilde{\eta}}_1 + k_{1,0}\tilde{\eta}_1 = 0 \tag{23a}$$

$$\dot{\tilde{\eta}}_2 + k_{2,0}\tilde{\eta}_2 = 0, \quad k_{i,j} > 0 \tag{23b}$$

Like (11) controller gains $k_{i,j}$ are determined by pole placement and the resulting control law including state feedback is given by:

$$u_{\text{A}} = \varphi_1(\eta_1, \dot{\eta}_1, \ddot{\tilde{\eta}}_{\text{ref},1} - k_{1,1}\dot{\tilde{\eta}}_1 - k_{1,0}\tilde{\eta}_1, \eta_2, \dot{\tilde{\eta}}_{\text{ref},2} - k_{2,0}\tilde{\eta}_2)$$
$$u_{\text{B}} = \varphi_2(\eta_1, \dot{\eta}_1, \ddot{\tilde{\eta}}_{\text{ref},1} - k_{1,1}\dot{\tilde{\eta}}_1 - k_{1,0}\tilde{\eta}_1, \eta_2, \dot{\tilde{\eta}}_{\text{ref},2} - k_{2,0}\tilde{\eta}_2)$$

## 4 Simulation Study

Since the objective of this work is the applicability of the controllers on a mobile hydraulic systems, the control performance is analyzed on the hydraulic system of a large material handler. To mimic the typical framework of controller hardware for mobile applications, the communication interval between controller and actuators is limited to $\Delta t = 10\,\text{ms}$. This influences the controller parametrization. For pole placement of the FTC (11) and input/output linearization (23) the numerical stability ranges of the solver have to be considered. In order to achieve conservative[4] stability for recursive Euler the poles $s_i$ are chosen in such a way that $|1 + \Delta t s_i| < 1$ holds. In particular, fixed step euler integration is used to simulate the sliding regime as other solvers result in integration error as stated by Utkin [28].
A challenging test regime (Fig. 2) with a rectangular load force profile with amplitude $F_{\text{L}} = 30\,\text{kN}$ is applied to evaluate the performance of the controllers.

[4] Other numerical integration methods possess larger and more complex stability areas [27]. For conservative stability the Euler stability range is considered.

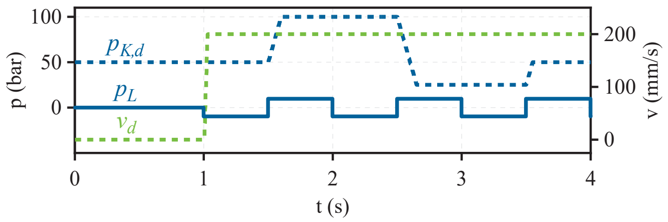


Figure 2 Test regime

### 4.1 Simulation models

Two models are created for validation and evaluation of the parametrized controllers. The simplified model is designed in *Matlab/Simulink* and mostly coincides with the model equations used for the controller design. Additionally, it includes measurement noise and nonlinear cylinder friction. Model simplifications are constant bulk modulus, no pressure drop across the pipes, constant supply pressure, neglected temperature influence, no valve dynamics and a linear valve opening characteristic.

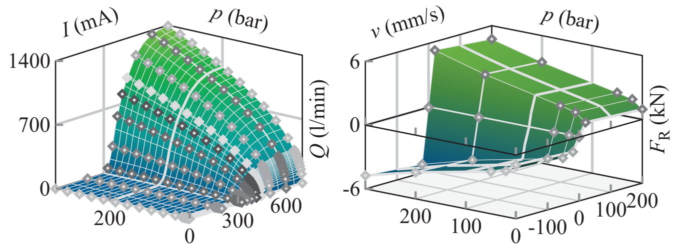


Figure 3 Valve flow characterstic (left) and nonlinear cylinder friction (right)

The complex model is based on the hydraulic system of a large two link mobile manipulator. The system modeled in *ETI ISI SimulationX* incorporates a complex hydraulic fluid model, realistic valve characteristics and friction models shown in Fig. 3. As with the simplified model the hydraulic pump is simplified and modeled as a constant pressure source.

### 4.2 Controller Adaption

During parametrization and evaluation of the controllers some minor adaptions were performed to enhance the controller performance: Firstly, to take into account the nonlinear valve orifice gradient in (3) a sixth degree polynomial is fitted to the valve characteristic and inverted for the control laws. And secondly, the error dynamics of the FTC (11) and input/output linearization (23) which originally incorporate proportional and derivative terms were extended by an integral error term, reducing static deviations through load force and other unmodeled influences.
We performed the controller parametrization using a cost function on trajectory tracking for each of the two controlled states. Parameter ranges were, if applicable obtained by definition equations 17 or pole placement, else determined empirically during simulation.

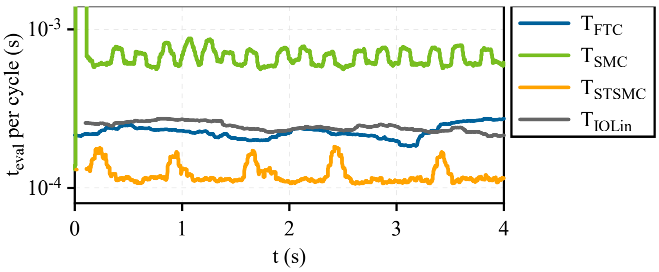


Figure 4 Computation time of controller per cycle

The design of the control laws of each of the four controllers requires complex symbolic computations as shown in Section 3. These were performed offline and the results are callable functions for online evaluation. As the expressions are very complex and lengthy the evaluation time per control cycle was measured during simulation (Fig. 4). The relevance of the absolute evaluation times is low as *Matlab* uses internal optimization and caching for faster evaluation, but it can be observed, that the SMC requires considerably more time per cycle to evaluate the control law than the other algorithms. This can be explained by the high switching frequency[5] at the sliding surface as zero-crossings present a common bottle-neck for function evaluation using discrete switching laws. The STSMC overcomes this issue by requesting

[5] The chattering in discrete time implementations of the SMC is caused by finite time switching limited to the sampling rate and not only a result of unmodeled dynamics [28].

$\dot{s} = 0$ and thus reducing chattering. This can be observed comparing velocity and pressure signals $(v, p_{\mathrm{K}})$ in Fig. 5b to 5c.

### 4.3 Controller Evaluation

Fig. 5a to 5d show the simulation results of the controlled states for the model validation $(v, p_{\mathrm{K}})$ and evaluation $(v^*, p^*_{\mathrm{K}})$. The simulation is initialized with prestressed chambers and the switching valve opens at $t = 1\,\mathrm{s}$.
On the simplified model all controllers achieve very satisfactory results on pressure control. Slight differences are observable at velocity tracking: While the FTC (Fig. 5d) shows little control errors and good disturbance rejection, the other controllers indicate slightly slower dynamics (Fig. 5a), small static errors and oscillations (Fig. 5b) and imperfect disturbance rejection (Fig. 5c). Generally speaking, independent control of $p_{\mathrm{K}}$ and $v$ was accomplished by all four controllers. However, the relatively slow communication frequency negatively affects the performance of the sliding regime controllers as the communication interval limits the switching frequency and thus introduces high frequency chattering.
Moving on to the manipulator's hydraulic system, significant increase of the control error can be observed on all four controllers. Only the combination of feed-forward control (21) and additional PID-like control through (24) of the FTC still obtains acceptable control results, though significant degradation in the form of overshooting and slower transient behavior is observable. The decoupling properties of the other algorithms are obviously reduced. This is especially problematic as the chamber pressure on both sides drops to $p_{\mathrm{T}} = 1\,\mathrm{bar}$ at the beginning of the motion thereby influencing the velocity tracking.

## 5 Conclusion

In this paper we evaluated four different control strategies for a nonlinear MIMO control problem. Specifically, the objective of this study was to investigate the applicability of these complex algorithms on mobile hydraulic systems. Challenging aspects in this field are parametric and model uncertainties, limited computational capacities and low communication frequency. Foundation for the model-based design is a simplified model of the valve controlled cylinder drive. This incorporates easily identifiable parameters such as geometric parameters as well as approximations of nonlinear model properties like friction and valve characteristic.

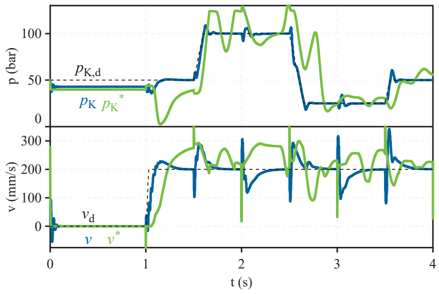


**(a)** Input/output linearization results for simple $(v, p_K)$ and complex hydraulic model $(v^*, p_K^*)$

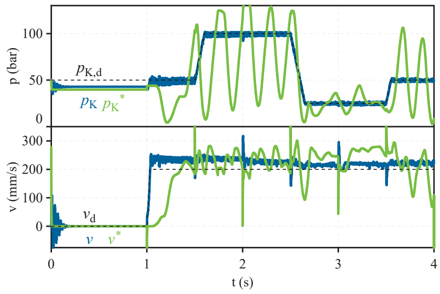


**(b)** SMC results for simple $(v, p_K)$ and complex hydraulic model $(v^*, p_K^*)$

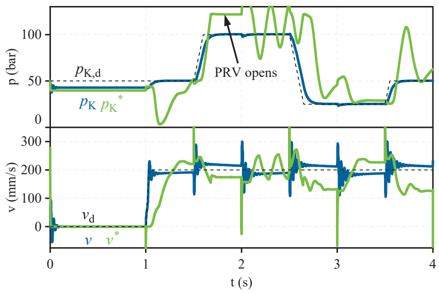


**(c)** STSMC results for simple $(v, p_K)$ and complex hydraulic model $(v^*, p_K^*)$. At approx. $1.6\,\text{s}$ the pressure relieve valve (PRV) opens as $p_B$ exceeds $370\,\text{bar}$.

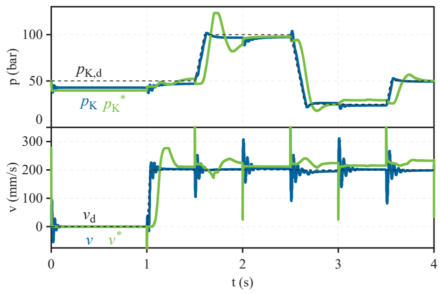


**(d)** FTC results for simple $(v, p_K)$ and complex hydraulic model $(v^*, p_K^*)$

Figure 5 Simulation results for velocity and weighted chamber control

Validation is performed on a simplified model, where the FTC and input/output linearization approach showed good follow-up behavior, disturbance rejection and decoupling of the two control variables. But also the sliding regime controllers reached satisfactory results with slight deterioration on the validation model.

Unfortunately, only one controller could reach comparable results on the more complex model. The deterioration was expected for input/output linearization approach as it depends on the inversion of the system model and is susceptible to model and parameter uncertainties. But also the more robust sliding mode controllers could not adequately control the given system. Main reason is the bandwidth limitation and deadtime of the actuating valves as real sliding theoretically requires infinitely fast actuators. Furthermore, the fixed communication time limits the switching frequency and thus creates chattering not due to unmodeled dynamics but due to discrete sampling. Only the flatness-based tracking controller achieved acceptable results. Although the feed-forward part of the controller is susceptible to parametric uncertainties and unmodeled dynamics, the additional linear controller is able to stabilize the system along the given trajectory.

We demonstrated in this study that a high modeling accuracy is mandatory for the considered control algorithms. Additionally, the low communication frequency of the controller poses a further source of chattering for the sliding based controllers and generally contributes to delayed control performance. However, these requirements are in contrast to the available resources. The controller design already requires the accurate measurement of the system output up to the second derivative. Qualified measurement results are highly questionable and more complex system models incorporating e.g. valve dynamics and variable bulk modulus will further increase the number of derivations necessary.

Lastly, the parametrization of the controllers represented a great challenge. Even though some control gains could be chosen by pole placement and with regard to the used sampling frequency others needed time-consuming empirical tuning with optimization tools.

## Acknowledgment

The work reported in this paper was performed within the project: “Development and testing of load- and motion-decoupled actuator structures using nonlinear, model-based control algorithms” funded by the DFG (German Research Society GZ: WE 4828/8-1 Transfer Project). The permission for publication is gratefully acknowledged.

Funded by DFG Deutsche Forschungsgemeinschaft German Research Foundation

## Nomenclature

| Designation | Denotation | [Unit] / Dim. |
|---|---|---|
| $A_\mathrm{A}, A_\mathrm{B}$ | Piston- and rod-side area of cylinder | $[\mathrm{m}^2]$ |
| $d_\mathrm{cyl}$ | Linear damping coefficient | $[\mathrm{s/m}]$ |
| $\boldsymbol{f}$ | Autonomous system part | $\mathbb{R}^n$ |
| $F_\mathrm{L}$ | External load force | [N] |
| $\boldsymbol{G}$ | Control-affine system part | $\mathbb{R}^{m\times p}$ |
| $\boldsymbol{h}$ | Output function | $\mathbb{R}^m$ |
| $h$ | Maximum cylinder stroke | $[\mathrm{m}]$ |
| $k_{i,j}$ | Control gains | [-] |
| $K'$ | Effective bulk modulus | [Pa] |
| $K_\mathrm{V}$ | Valve orifice gradient | $[\mathrm{m}^3\mathrm{s/kg}]$ |
| $m_\mathrm{cyl}$ | cylinder mass | [kg] |
| $p_\mathrm{A}, p_\mathrm{B}$ | Chamber pressure | [Pa] |
| $p_\mathrm{K}$ | Weighted chamber pressure | [Pa] |
| $p_{i,\mathrm{d}}$ | Desired pressure | [Pa] |
| $p_0$ | Supply pressure | [Pa] |
| $p_\mathrm{T}$ | Reservoir pressure | [Pa] |
| $Q_\mathrm{A}, Q_\mathrm{B}$ | Flow | $[\mathrm{m}^3/\mathrm{s}]$ |
| $r_i$ | Relative degree | [-] |
| $s_i$ | Sliding surface | [-] |
| $\boldsymbol{u}$ | Controller Output / System input | $\mathbb{R}^p$ |
| $\boldsymbol{x}$ | System state | $\mathbb{R}^n$ |
| $\boldsymbol{y}$ | General system output | $\mathbb{R}^m$ |
| $v_\mathrm{d}$ | Desired cylinder velocity | $[\mathrm{m/s}]$ |
| $V_\mathrm{A}, V_\mathrm{B}$ | Constant pipe volume | $[\mathrm{m}^3]$ |
| $z$ | Cylinder position | $[\mathrm{m}]$ |
| $\pounds$ | Lie-derivative | [-] |
| $\epsilon$ | Saturation dead zone | [-] |
| $\boldsymbol{\eta}$ | Flat system output | $\mathbb{R}^m$ |
| $\eta$ | Control parameter for asymptotic convergence towards sliding surface | [-] |
| $\lambda$ | Control parameter for exponential convergence on sliding surface | $[1/\mathrm{s}]$ |
| $\varphi_i$ | Transformation between flat output and input | [-] |
| $\boldsymbol{\psi}$ | Transformation between flat output and state | [-] |
| $\boldsymbol{\omega}$ | Virtual control input | [-] |

## References

[1] G. Kolks and J. Weber, "Modiciency-Efficient industrial hydraulic drives through independent metering using optimal operating modes," in *Proc. of the 10th International Fluid Power Conference (10. IFK)*, vol. 1, Dresden, 2016, pp. 105–120.

[2] J. Lübbert, A. Sitte, and J. Weber, "Neue Lösungen für elektrohydraulische Steuerungssysteme mobiler Arbeitsmaschinen mit aufgelösten Steuerkanten," DFG, Final Report WE 4828/1-1, May 2016.

[3] Volvo CE Europe, "Large Crawler Excavators: Volvo EC530E/EC550E," Jul. 2021. [Online]. Available: https://www.volvoce.com/europe/en/products/excavators/ec550e/

[4] A. Sitte and J. Weber, "Structural design of independent metering control systems," in *Proc. of the 13th Scandinavian International Conference on Fluid Power*. Linköping, Sweden: Linköping University Electronic Press, 2013, pp. 261–270.

[5] A. Sitte, B. Beck, and J. Weber, "Design of independent metering control systems," in *Proc. of the 9th International Fluid Power Conference*, Aachen, 2014.

[6] A. Isidori, A. J. Krener, C. Gori-Giorgi, and S. Monaco, "Nonlinear Decoupling via Feedback: A Differential Geometric Approach," in *Proc. of IEEE Transactions on Automatic Control*, vol. 26, no. 2, 1981, pp. 331–345.

[7] A. J. Krener, A. Isidori, and W. Respondek, "Partial and Robust Linearization by Feedback," in *Proc. of the 22nd IEEE Conference on Decision and Control*, 1983, pp. 126–130.

[8] A. Isidori, "Exact Linearization Methods," in *Nonlinear control systems*, 1st ed. Berlin: Springer, 1985, pp. 178–253.

[9] T. I. Fossen and B. A. Foss, "Sliding Control of MIMO Nonlinear Systems," *Modeling Identification and Control*, vol. 12, no. 3, pp. 129–138, 1991.

[10] V. I. Utkin, *Sliding modes in control and optimization*, 1st ed. Berlin: Springer DE, 1992.

[11] J.-J. E. Slotine and S. S. Sastry, "Tracking Control of non-linear systems using sliding surfaces, with application to robot manipulators," *International Journal of Control*, vol. 38, no. 2, pp. 465–492, 1983.

[12] K. D. Young, V. I. Utkin, and U. Özgünür, "A control engineers guide to sliding mode control," in *Proc. of IEEE Transactions on Control Systems Technology*, vol. 7, no. 3, 1999, pp. 328–342.

[13] J.-J. E. Slotine and W. Li, *Applied Nonlinear Control*. Englewood Cliffs, New Jersey: Prentice Hall, 1991.

[14] A. Levant, "Sliding order and sliding accuracy in sliding mode control," *International journal of control*, vol. 58, no. 6, pp. 1247–1263, 1993.

[15] L. Fridman and A. Levant, "Higher order sliding modes as a natural phenomenon in control theory," in *Robust control via variable structure and Lyapunov techniques*. London: Springer, 1996, pp. 107–133.

[16] G. Bartolini, A. Ferrara, E. Usai, and V. I. Utkin, "On Multi-Input Chattering-Free Second-Order Sliding Mode Control," in *Proc of IEEE Transactions on Automatic Control*, vol. 45, no. 9. IEEE, 2000, pp. 1711–1717.

[17] J. Davila, L. Fridman, and A. Levant, "Second-Order Sliding-Mode Observer for Mechanical Systems," in *Proc. of IEEE Transactions on Automatic Control*, vol. 50, no. 11, 2005, pp. 1785–1789.

[18] J. Rivera, L. Garcia, C. Mora, J. J. Raygoza, and S. Ortega, "Super-Twisting Sliding Mode in Motion Control Systems," *Sliding Mode Control*, vol. 1, pp. 237 – 254, 2011.

[19] J. A. Moreno and M. Osorio, "Strict Lyapunov Functions for the Super-Twisting Algorithm," in *Proc. of IEEE Transactions on Automatic Control*, vol. 4, no. 57, 2012, pp. 1035–1040.

[20] T. Gonzalez, J. A. Moreno, and L. Fridman, "Variable gain super-twisting sliding mode control," in *Proc. of IEEE Transactions on Automatic Control*, vol. 57, no. 8, 2012, pp. 2100–2105.

[21] M. Fliess, J. Lévine, P. Martin, and P. Rouchon, "On differntially flat nonlinear systems," in *Nonlinear Control Systems Design 1992*, Bordeaux, France, 1992, pp. 159–163.

[22] R. Rothfuß, "Application of flatness-based analysis and control of nonlinear MIMO systems," PhD thesis, 1997. [Online]. Available: http://dx.doi.org/10.18419/opus-4118

[23] R. Bindel, R. Nitsche, R. Rothfuß, and M. Zeitz, "Flatness Based Control of a Two Valve Hydraulic Joint of a Large Manipulator," in *Proc. of IEEE European Control Conference (ECC)*, Karlsruhe, Germany, 1999, pp. 3190–3195.

[24] G. Kolks and J. Weber, "Controller Design for Precise and Efficient Industrial Cylinder Drives Using Independent Metering Valves," in *Proc. of the 9th FPNI Ph.D. Symposium on Fluid Power*, vol. 50473. Florianópolis, SC, Brazil: ASME, 2016.

[25] K. Röbenack, *Nichtlineare Regelungssysteme - Theorie und Anwendung der exakten Linearisierung*, 1st ed. Springer Vieweg, 2017.

[26] I. Nagesh and C. Edwards, "A multivariable super-twisting sliding mode approach," *Automatica*, vol. 50, no. 3, pp. 984–988, 2014.

[27] K. Janschek, *Systementwurf mechatronischer Systeme*. Springer, 2010, vol. 1.

[28] V. I. Utkin, A. Poznyak, Y. V. Orlov, and A. Polyakov, "Discrete-Time Systems," in *Road Map for Sliding Mode Control Design*. Springer, 2020, vol. 1, no. SpringerBriefs in Mathematics, pp. 91–97.


## Biography

**Lukas Bachmann** is a research assistant at TUD University of Technology Dresden, where he has been working at the Chair of Fluid-Mechatronic systems since 2021. He holds a diploma engineer degree in electrical engineering from the TUD University of Technology Dresden. His areas of expertise include nonlinear control theory, automation, robotics and multi-domain simulation. At the Chair of Fluid-Mechatronic systems, as leader of the mobile applications group, his current studies are focused on control and automation of mobile hydraulic systems incorporating independent metering valve technology.